Proceedings of the IASS 2024 Symposium
Redefining the Art of Structural Design
August 26-30, 2024, Zurich Switzerland
Philippe Block, Giulia Boller, Catherine DeWolf,
Jacqueline Pauli, Walter Kaufmann (eds.)

Geometry, material, and structural exploration for curved cross-laminated timber structures

Juan S. ZAMBRANO-JARAMILLO[a], Erica C. FISCHER[a], Dylan WOOD*

*University of Oregon
318 Lawrence Hall, Eugene, OR
dmwood@uoregon.edu

[a] Oregon State University, College of Engineering, Civil and Construction Engineering

Abstract

Cross-laminated timber (CLT) has become a widely used wood product in walls, floors, and roof structures due to its high stiffness, relatively low weight, and ecological benefits of timber as a building material. Even though wood can be elastically bent and laminated into curved surfaces, the structural benefits of curvature are rarely in wood panel products. This problem is in part because of the complications of incorporating aspects of the material, geometry, manufacturing, and architectural constraints into a holistic workflow. To tackle this problem, we present a digital workflow for evaluating, exploring, and optimizing the use of single curved CLT surface geometries. The workflow consists of a parametric, geometric model, and a Finite Element Model (FEM) that is linked to automate and plot the structural results and the architectural geometry. Using this method and an optimization routine, we can identify structurally favorable geometries that reduce overall material use while considering the lamella thicknesses and fiber orientations required for manufacturing. The workflow was tested using a simple barrel-vaulted ceiling/floor slab with the dimension of a typical CLT panel, identifying the combination of viable curvatures and cross-sections that reduce material compared to a flat CLT panel product.

Keywords: Curved timber panel, Rhino-Grasshopper, Abaqus, Cross-laminated timber, Panel optimization.

1. Introduction and background

Structural design consists of an iterative process such that architectural and engineering design can achieve a balance between functionality, appearance, performance, and material efficiency in contemporary construction. These iterations can be time consuming and therefore costly, particularly with modern architectural geometries. When design platforms between the architect and engineer are not integrated, substantial delays in the planning and design phases of the project can occur [1].

Elongated design phase schedules can delay time to having occupants within a building and therefore revenue for the owners. As contemporary construction becomes more complex, interaction between the design team is essential to minimize the duration of the design phase. Back-and-forth communication becomes more cumbersome as complex structural details are required to satisfy geometric irregularities. Architectural software like Rhino/Grasshopper has developed advanced modeling techniques that involve parametric modeling to handle the project design phase [1], [2]. Architects use this software to facilitate the translation of ideas that come from natural inspiration into building forms [3], [4], [5]. However, the structural engineering behind those irregular elements requires additional analysis to guarantee the capacity and serviceability of such irregular geometry.

Even though modeling techniques have developed at the same speed as modeling software capabilities, architectural modeling software cannot consider the effect of material capacity on irregular geometries.

These analysis limitations can be overcome by coupling different software to fill the gaps and complement the numerical simulation with additional results that verify the structural performance. Some Building Information Modeling (BIM) software like Revit have been linked to Finite Element (FE) software like SAP200 to obtain the structural response [6], [7]. For complex geometries such as curved shell elements, a more specialized and computationally powerful FE software (e.g. Abaqus) is necessary for parametric research studies based on the extensive and diverse element library available for modeling the curved surfaces using solid or shell elements [8], [9], [10].

Different methodologies have been used to couple geometric modeling software (e.g. Rhino/Grasshopper) and structural FE software (e.g. Abaqus). Models created in Rhino have been coupled with Catia, Hypermesh, Midas, Ansys, or Abaqus [12]; other cases generated the initial geometry in Rhino/Grasshopper to pre-process the input structural model with Autodesk plugins and then executed them using Abaqus [11], [12]. For irregular shapes constructed with 3D printed concrete, Rhino/Grasshopper was used to generate the models and create the input file to execute the structural analysis using Abaqus, which were compared and calibrated with experimental tests [13], [14]. Additional cases included other programming languages to create interfaces between AutoCAD through MATLAB or Python with Rhino/Grasshopper and FE software like SAP2000 and Abaqus [15], [16], [17].

The coupling approach of architectural modeling software and structural analysis allows for design and research teams to evaluate structures on multiple performance objectives thereby analyzing for optimization. Principal Component Analysis (PCA) [18], [19], [20] can be utilized to process large groups of variables to obtain the results as part of a whole system. The primary purpose of PCA is to identify correlations between a set of variables, or in this case, relations between complex model geometric parameters and the performance objectives being analyzed. Researchers applied these optimization methodologies directly to architectural and engineering fields for shape, architectural functionality, or structural performance optimization [21], [22], [23], [24].

2. Research objectives

This paper provides a methodology of coupling architectural modeling software, Grasshopper/Rhino and structural analysis FE modeling software, Abaqus, to optimized curved cross laminated timber geometries. By coupling these software, the analysis does not require assumptions or modifications in terms of the model geometry compared to the cases where the numerical models are redefined in the FE software to simulate the behavior of the structure. In this case, any geometric interaction between different parts of the structure will be included in the analysis by considering the actual model shape.

Cross laminated timber (CLT) is constructed from timber, a renewable resource, and has become popular in construction in recent years due to its sustainability performance and biophilic nature. Therefore, often volume of material is a key performance metric on CLT projects that often competes with the structural performance for large open floor plans. An optimization methodology was designed to consider the structural behavior of CLT panels in one-way bending, the volume of the material being considered, and the radius of curvature of the CLT in the structure. By evaluating a single panel, the basic cross section of the curved panel is assessed to define the optimal configuration that balances architectural and engineering objectives.

3. Methodology

3.1. Coupling of modeling software

The first stage of the study analyzed different methods available to import the geometry of curved surfaces modeled in Rhino/Grasshopper [14], [15], [16], [17]. Two methods were defined based on the output file from Rhino/Grasshopper (Figure 1). The first methodology required a text file with the coordinates of the boundary points of the curved shells modeled in Rhino/Grasshopper. After that, the points were filtered to classify and organize them into data sets to define independent curves. A Python script was generated with the input values and executed in Abaqus to create a spline with each data set. A shell loft was created as part of the script to complete the model and assign the boundary conditions

for the analysis before solving the FE problem. The second methodology was based on a STEP file containing information on the entire surface modeled in Rhino/Grasshopper. This methodology provides the complete model part for the assembly as it was originally modeled. A Python script was generated to load the geometry and define the properties and boundary conditions. The script was executed in Abaqus to assign all the properties, and the FE problem was solved similar to the first methodology. To obtain the results, a Python script was developed to write the output into text files for post-processing and evaluate any optimization procedure.

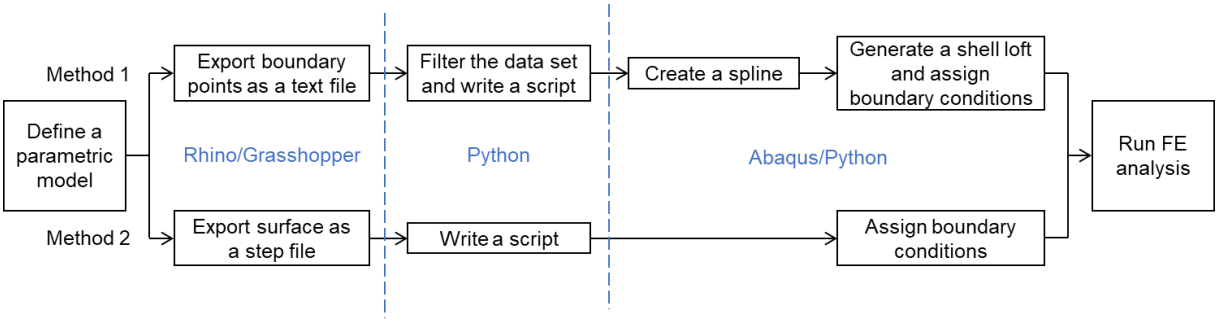

Figure 1: Workflow of the automatization process defined to analyze the curved panels.

3.2. Optimization framework

An optimization framework was developed to evaluate a corner-supported curved panel 8 m in length with a width-to-length ratio of 1:4. The structure was assumed to be a roof structure (Figure 2) with uniformly distributed dead load and live load applied normal to the panel surface. Three performance objectives were considered: material efficiency, structural performance, and service level. Each objective is evaluated by one parameter, such as the volume of timber, maximum stress, and deflection limits of the panel, respectively (Table 1). The optimization framework was developed around this case and will be applied to more complicated geometries in the future.

Table 1: Performance objectives

Objective	Metric	Evaluation Method
Material efficiency	Volume of timber	Member sizing
Structural performance	Maximum stress	FEM
Service level	Deflection limit	FEM

The CLT panels' cross-section was assessed based on the number of plies, categorized into three groups of 3-, 5-, and 7-ply panels with *(n-1)/2* longitudinal plies and *(n+1)/2* transversal plies. Longitudinal plies overlapped with the transversal plies; the transversal plies were always the top and bottom plies. Although the panel's thickness was adjustable, the transverse plies, oriented in the short span, were fixed at 10mm due to the curved panel's construction constraints. For each group, the longitudinal plies, oriented in the long span, were determined and ranged from t_i = 10mm to t_i = 50mm, with a 10mm increment. Each ply was arranged in an alternating pattern to define the panel cross-section, with the top and bottom plies always oriented in the short span (Figure 2).

All models in the analysis were based on an orthotropic elastic material. The elastic modulus, Poisson ratios, and shear modulus for each direction were described in Table 2. To estimate the demand capacity ratio (DCR) of the panels under gravity load, the strength properties of grade V1 were used ANSI/APA PRG 320-2019 [25]. To evaluate the service performance of the panels, a limit of L/240 was defined as recommended for roof elements ASCE7-22 [26]. During the analysis, the self-weight of the panels was considered, in addition to the roof live load and snow load.

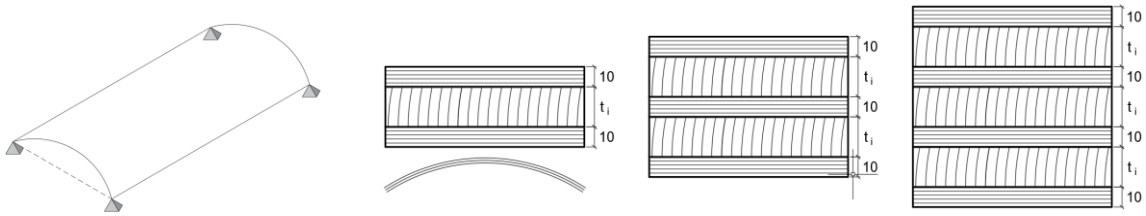

(a) (b)

Figure 2: a) Boundary conditions for a general panel configuration, and b) Cross-section configuration of the panels (3-, 5-, and 7-ply).

Table 2: Elastic properties of orthotropic material.

Elastic material		**Strength limit**	
E_1 [MPa]	13530	F_{t1} [MPa]	3.96
E_2 [MPa]	920	F_{c1} [MPa]	9.31
E_3 [MPa]	676	$F_{t2,3}$ [MPa]	2.24
μ_{12} [-]	0.292	$F_{c2,3}$ [MPa]	5.34
μ_{13} [-]	0.449	F_v [MPa]	1.24
μ_{23} [-]	0.390		
G_{12} [MPa]	866		
G_{13} [MPa]	1055		
G_{23} [MPa]	95		

The output parameters for the single panel consider three main properties. The first parameter was the volume of the panel, which is inversely proportional to the radius of curvature. The second parameter was the panel vertical deflections at three main points (Nodes B, D, and E) (Figure 3). The third output of the analysis was the normal stresses and shear stress, all at the top and bottom of the panels, at four main points (Node A, B, D, and E). Other points were not included due to the symmetry of the curved panel.

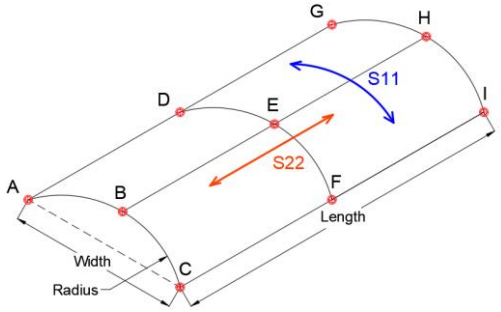

Figure 3: Nodes and stresses distribution for output parameters of a single panel.

To define the optimum panel configuration, each performance objective was graded in a range from 0 to 1. First, all the outcomes were normalized for comparison; the volume of timber was normalized with the volume of a flat 3-ply panel having a value of 1 (the least amount of timber required for the given surface) and the 7-ply panel with a total thickness of 190 mm and radius of curvature of 1400 mm with a value of 0 as it used the largest volume of timber. The material efficiency objective considered only the volume of timber; its performance was evaluated with the other objectives.

The vertical deflection was independently normalized for each node where it was calculated, assigning a value of 1 to the node with the smallest deflection within the entire data set of the three different ply layups to allow comparison between panels of different numbers of plies. Similarly, a value of 0 was assigned to the node with the largest vertical deflection for the entire data set of the same node. The performance value for the service level objective was calculated as the average of the normalized values

from nodes B, D, and E. The flat panel was not included in the normalization process of the vertical deflections because the flat panel represents an extreme value for the distribution.

The DCR was calculated based on the strengths provided in Table 2 for the stresses in the panel. Each direction and location, either the top or bottom of the panel, was normalized independently between the entire data set of the three different ply layups to allow comparison between panels of different numbers of plies. A value of 1 was assigned to the case with the smallest DCR and a value of 0 to the largest DCR. Similarly to the vertical deflection, the flat panel was not included in the normalization process because the stresses in the flat panel represent an extreme value for the distribution. The structural performance was calculated as an average of the performance of each node (A, B, C, and D), considering the top and bottom location and each stress orientation (S11, S22, and S12, Figure 3).

After calculating the independent performance objectives, each normalized value was assigned to an orthogonal axis of a three-dimensional space (Figure 4). To obtain a single performance value for general comparison, the volume of the triangular pyramid formed between the performance objectives and the origin was calculated to obtain a single value to rank the performance of the curved panels based on their efficiency. The cases that generate the largest volume were considered as the most efficient as they combine the results from each performance objective.

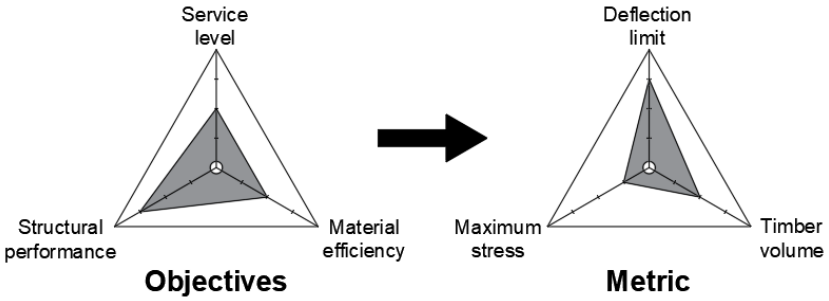

Figure 4: Performance objectives for the curved panels.

4. Results

To analyze the panels, input parameters were defined to develop a Python script for Abaqus. Each numerical model featured different thicknesses of longitudinal plies, with constant length and width. Seven radii of curvature were analyzed, with the smallest and largest radius serving as limits for the intermediate cases. Intermediate values were determined by equally spacing the minimum and maximum curvature radius based on panel height. The analyzed radius values included 1400 mm, 1509 mm, 1651 mm, 1838 mm, 2092 mm, 2454 mm, and 3000 mm. A flat panel (curvature radius equal to $1x10^6$ mm) was also included as a base case to compare the timber volume required for each curved panel.

The numerical model was developed in Abaqus as a 3D extruded shell based on the radius of curvature provided. The material properties were elastic during the entire analysis, and the strength limits provided in Table 2 were used for further comparison. A composite shell section was assigned with the required number of plies, and their thickness and orientation were assigned for the longitudinal and transversal plies. The analysis was performed as static, with the self-weight loaded as the density for the material, and the live load and snow load were applied as a distributed load perpendicular to the panels' surface. The mesh size was 200 mm. The control points were defined to verify and obtain displacements and stresses from the numerical models.

4.1. Volume of timber

The panels were classified into three groups based on the number of plies assigned. This classification was used for comparison because the performance values were calculated considering all the groups as part of the same data set to analyze all the panels under the same parameters. If each group of panels is compared independently, the panel with the smaller radius of curvature (1400 mm) requires 11.4% more timber than a flat panel. The increase in the volume of timber for each radius of curvature is shown in Table 3 where the *volume rate* is the percent increase in volume of timber as compared to a flat panel.

Table 3: Increment of volume ratio for a single panel group.

Radius [mm]	1400	1509	1651	1838	2092	2454	3000	$1x10^6$
Volume rate [%]	11.4	9.3	7.4	5.7	4.3	3.0	2.0	0.0

4.2. Vertical deflections

Vertical deflections were measured at three nodes (B, D, and E), and the behavior was similar for all groups. The cases with thicker plies and smaller radius satisfy the deflection limit for the imposed loads. The bending effect in the short direction reduces the deflection at node E with respect to node D. This effect was seen in the 3-ply panels and less proportion for the 5-ply panels. (See t = 50 mm cases with r = 1400 mm in Figure 5). Even though most of the panels do not satisfy the limit deflection ratio, the relationship between the responses was still acceptable for estimating the performance of the panels. The material was considered elastic, therefore Figure 5 shows that deflections and load capacity are limiting design parameters for the design of curved panels. If the applied load were reduced, the relation would remain linear to satisfy the deflection limits.

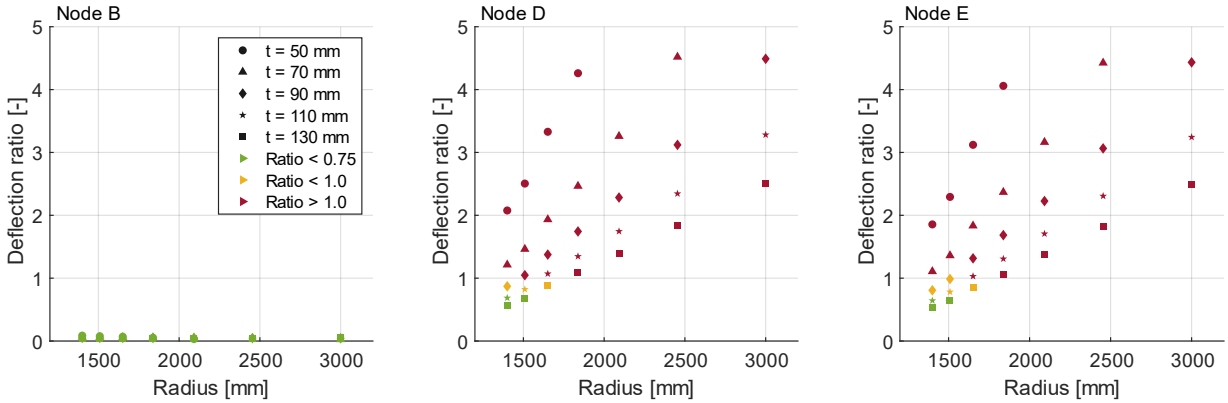

Figure 5: Vertical deflection ratio for 5-ply panels.

4.3. Maximum stress

All the curved panels showed a similar stress distribution (Tension = Red, Compression = Blue, Figure 6 and Figure 7) based on the assigned orientations (Figure 3). The S11 stresses are the primary bending stresses in the short direction of the panel, the S22 stresses are the primary bending stresses in the long direction of the panel, and the S13 stresses are the shear stresses in the panel. For the S11 orientation of the model, the top fibers at the center are in tension (Figure 6a). This effect was increased for a smaller radius of curvature due to the application of a distributed load normal to the surface at the top of the panel. This is the same effect that produces lower vertical deflections at node E compared to node D. The S22 orientation corresponds to the long-span distribution, for which the curved panel shows the same distribution of a simply supported beam with tension at the bottom fibers and compression at the top fibers (Figure 6b). Regarding the shear stresses, Figure 6c and Figure 7 (Node A, orientation S12) show some stress concentrations at the corners of the panel, which are related to the boundary conditions assigned as fixed on a single point.

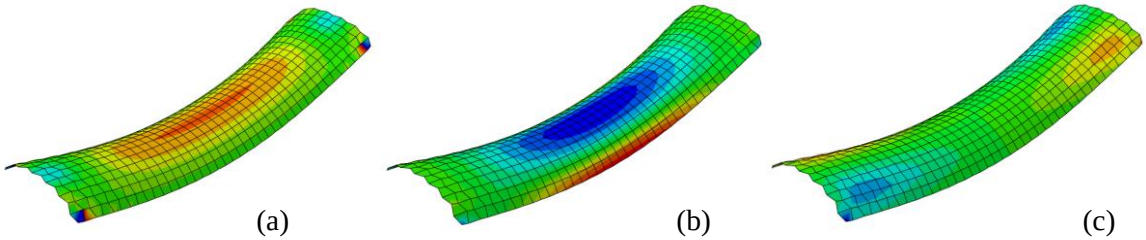

Figure 6: FE model deformed shape and stress distribution: a) S11, b) S22, and c) S13.

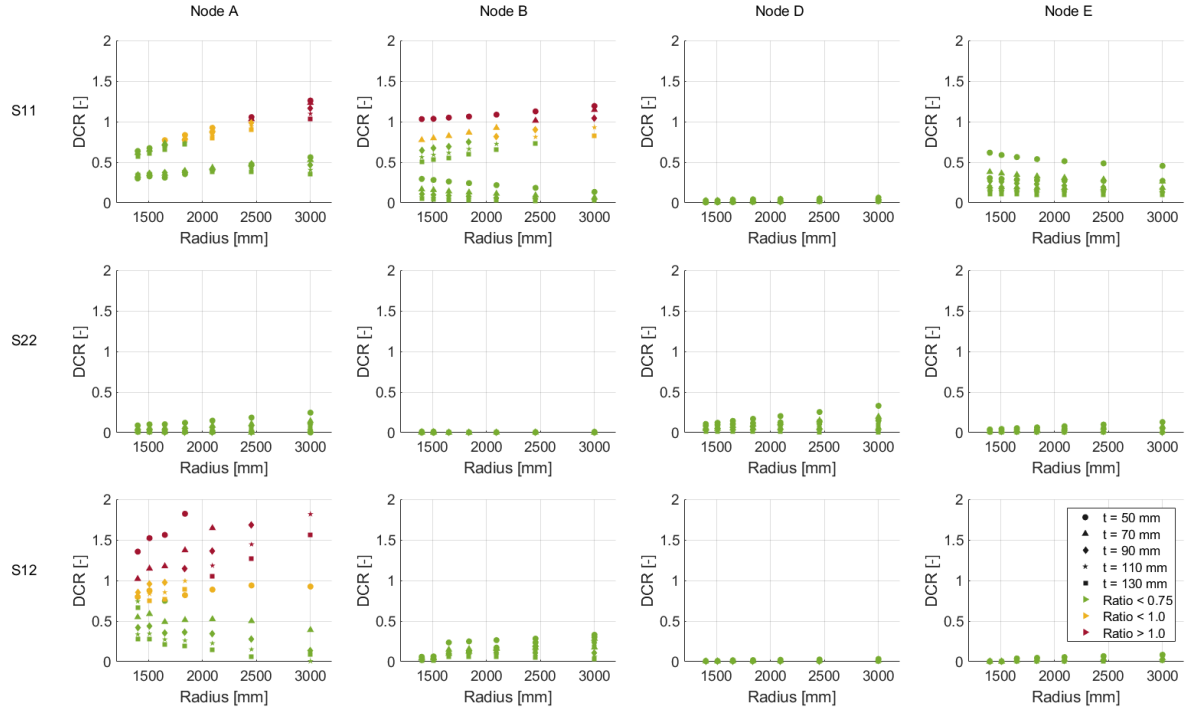

Figure 7: DCR classified per node location and stress orientation of the 5-ply panels.

4.4. Optimization process

The results from each performance objective were normalized with the values from all the panels, and the results (range between 0 to 1) were plotted in 3D to generate a triangular pyramid with the origin. The volume of the pyramid represents the global performance of the panels (Figure 8), where if one of the performance objectives received a low grade, the general performance is affected proportionally to the normalized values. Figure 8 shows the cases for the 3-ply panels, for each row from left to right; when the radius of curvature increased (curvature reduction), the material efficiency was increased due the reduction of timber volume, however the service level (vertical deflection) and structural performance (bending stress) objectives reduced their efficiency with the increase of the radius of curvature. Equivalently, for each column in Figure 8, from the top to the bottom, as the thickness of the panels increased, the material efficiency decreased due the increase of timber volume; however, the service level and structural performance objectives increased their efficiency as the maximum stresses and vertical deflections were reduced.

As a summary of the behavior of the curved panels with variable radius of curvature, variable thickness, and different numbers of plies, Figure 9 shows a comparable response in all the cases. For 3-ply panels, the optimum cases are the panels with the smallest radius of curvature independent of their thickness. For the 5- and 7-ply panels, when the thickness of the panels is required to be larger, the optimum cases are the intermediate radius analyzed. In addition, as a global result, panels with a total thickness between 50 to 70 mm are the ones that show a better performance, independent of the number of plies.

Table 4 describes the best cases for each of the cross-section configurations. As mentioned before, panels with thicknesses between 50 and 70 mm have the best global performance. The fabrication cost should be the final variable to determine which alternative is more efficient and economically reasonable for the design of bigger structures. However, that is out of the scope of the current research.

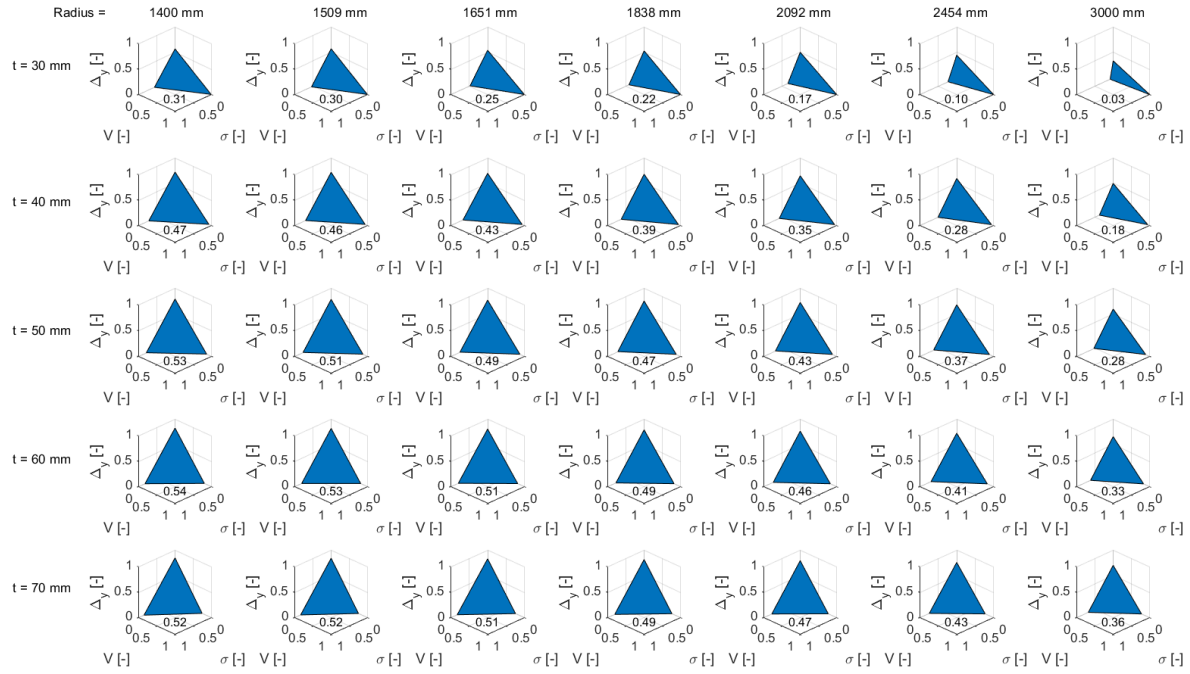

Figure 8: Normalized performance ratios for stresses (σ – X axis), volume of timber (V – Y axis), and vertical deflections (Δ_y – Z axis) of the 3-ply panels.

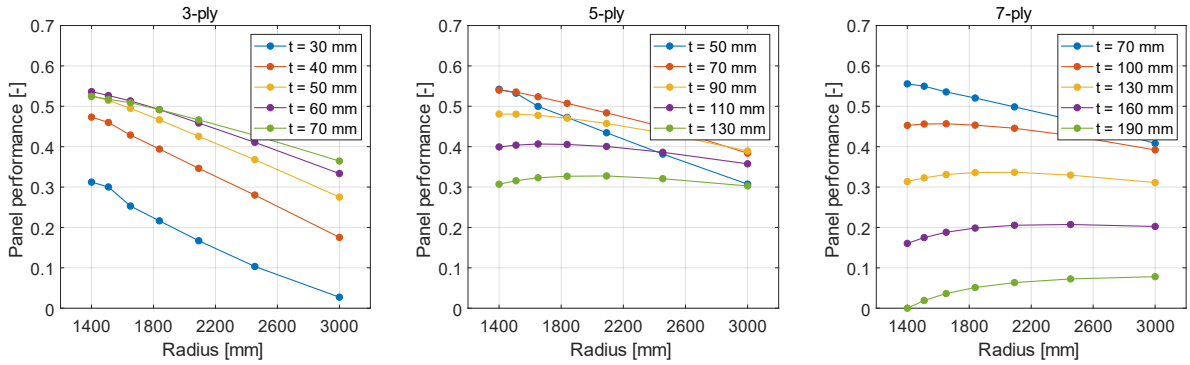

Figure 9: Panel performance as a function of normalized stresses, timber volume, and vertical deflections for 3-, 5-, and 7-ply panels.

Table 4: Summary of the best performance cases based on the number of plies

Number of plies	t [mm]	Vol [m3]	Performance objectives			Global performance [-]
			Volume [-]	Deflections [-]	Stress [-]	
3	60	1.07	0.80	0.82	0.82	0.54
5	50	0.89	0.86	0.81	0.78	0.54
7	70	1.25	0.74	0.87	0.87	0.56

5. Conclusions and future work

This paper provides a framework for coupling modeling software used in the architectural field with powerful commercial FE software to analyze the structural performance of a curved CLT structure and an optimization framework to balance architectural features with structural performance. This process reduces the uncertainties generated by simplifications or modifications in the geometry for the FE model. Using Python scripts to generate the numerical model from the boundary points of the curved structures

or to import the entire surfaces results in an easier and convenient solution to perform parametric analyses with multiple iterations.

For the optimization process, each performance objective (Table 1) was analyzed independently, and the results were combined to obtain the global performance of the curved panels. In terms of the timber volume, if the number of plies was constant, the maximum increment of timber volume was 11.4% compared to the flat panel. However, to use a flat panel, it was necessary to reduce the span or include longitudinal beams to give support to the element as traditional construction methods to satisfy the performance objectives.

Vertical deflections were defined as important parameters that limit the maximum applied load and control the curved panel's design. In addition, the maximum vertical deflections were located at the border of midspan as the center point tends to have lower deflections due to the transversal bending effect caused by the applied distributed loads normal to the panel surface. The stress distribution in the panels was similar for all the cases, and it was also considered as a limiting factor for the design to reduce the maximum applied load based on the material strength.

Next steps in this research will include analyzing a bigger structure modeled with curved cross-laminated timber panels to generalize the interaction between the parametric modeling software and the FE software. In addition, with a bigger structure, panel optimization will be applied to determine the interaction of different surfaces and develop a methodology to include the connections between the panels.

Acknowledgements

This research is funded by the USDA Research Service (ARS), grant number 58-0204-6-002. Thank you to Braden Lawrie for his contribution with the architectural models developed in Rhino/Grasshopper in this project.

References

[1] R. Chairiyah, A. E. Yetti, and I. Pujiyanti, "The Grasshopper+Rhino for 3D Modelling in Indonesian's Education of Biomimetic Architecture:," presented at the International Webinar on Digital Architecture 2021 (IWEDA 2021), Yogyakarta, Indonesia, 2022. doi: 10.2991/assehr.k.220703.041.

[2] M. Stavric and O. Marina, "Parametric Modeling for Advanced Architecture," vol. 5, no. 1, 2011.

[3] M. Alshami, M. Atwa, A. Fathy, and A. Saleh, "Parametric Patterns Inspired by Nature for Responsive Building Façade," *Int. J. Innov. Res. Sci. Eng. Technol.*, vol. 4, no. 9, pp. 8009–8018, Sep. 2015, doi: 10.15680/IJIRSET.2015.0409002.

[4] M. Helenowska-Peschke, "APPLYING GENERATIVE MODELLING TOOLS TO EXPLORE ARCHITECTURAL FORMS," vol. 23, 2012.

[5] L. Kormaníková, E. Kormaníková, and D. Katunský, "Shape Design and Analysis of Adaptive Structures," *Procedia Eng.*, vol. 190, pp. 7–14, 2017, doi: 10.1016/j.proeng.2017.05.300.

[6] A. S. Hadi, A. M. Abd, and M. Mahmood, "Integrity of Revit with structural analysis softwares," *IOP Conf. Ser. Mater. Sci. Eng.*, vol. 1076, no. 1, p. 012119, Feb. 2021, doi: 10.1088/1757-899X/1076/1/012119.

[7] R. Ren, J. Zhang, and H. N. Dib, "BIM Interoperability for Structure Analysis," in *Construction Research Congress 2018*, New Orleans, Louisiana: American Society of Civil Engineers, Mar. 2018, pp. 470–479. doi: 10.1061/9780784481264.046.

[8] T. S. Lau and S. H. Lo, "Finite element mesh generation over analytical curved surfaces," *Comput. Struct.*, vol. 59, no. 2, pp. 301–309, Apr. 1996, doi: 10.1016/0045-7949(95)00261-8.

[9] B. Meyghani, M. Awang, and C. S. Wu, "Finite element modeling of friction stir welding (FSW) on a complex curved plate," *J. Adv. Join. Process.*, vol. 1, p. 100007, Mar. 2020, doi: 10.1016/j.jajp.2020.100007.

[10] A. J. Sadowski and J. M. Rotter, "Solid or shell finite elements to model thick cylindrical tubes and shells under global bending," *Int. J. Mech. Sci.*, vol. 74, pp. 143–153, Sep. 2013, doi: 10.1016/j.ijmecsci.2013.05.008.

[11] Y. Lai, L. Liu, Y. J. Zhang, J. Chen, E. Fang, and J. Lua, "Rhino 3D to Abaqus: A T-Spline Based Isogeometric Analysis Software Framework," in *Advances in Computational Fluid-Structure Interaction and Flow Simulation*, Y. Bazilevs and K. Takizawa, Eds., in Modeling and Simulation in Science, Engineering and Technology. , Cham: Springer International Publishing, 2016, pp. 271–281. doi: 10.1007/978-3-319-40827-9_21.

[12] Y. Lai, Y. J. Zhang, L. Liu, X. Wei, E. Fang, and J. Lua, "Integrating CAD with Abaqus: A practical isogeometric analysis software platform for industrial applications," *Comput. Math. Appl.*, vol. 74, no. 7, pp. 1648–1660, Oct. 2017, doi: 10.1016/j.camwa.2017.03.032.

[13] G. Vantyghem, T. Ooms, and W. De Corte, "VoxelPrint: A Grasshopper plug-in for voxel-based numerical simulation of concrete printing," *Autom. Constr.*, vol. 122, p. 103469, Feb. 2021, doi: 10.1016/j.autcon.2020.103469.

[14] G. Vantyghem, T. Ooms, and W. De Corte, "FEM MODELLING TECHNIQUES FOR SIMULATION OF 3D CONCRETE PRINTING," 2020.

[15] L. I. W. Arnouts, T. J. Massart, N. D. Temmerman, and P. Z. Berke, "Structural optimisation of a bistable deployable scissor module," 2019.

[16] A. Baghdadi, M. Heristchian, and H. Kloft, "Displacement-based seismic assessment of Heinz Isler's shell structures," Aug. 2021.

[17] N. Wonoto and V. Blouin, "Integrating Grasshopper and Matlab for Shape Optimization and Structural Form-Finding of Buildings," *Comput.-Aided Des. Appl.*, vol. 16, no. 1, pp. 1–12, Aug. 2018, doi: 10.14733/cadaps.2019.1-12.

[18] J. Sobieszczanski-Sobieski, "Multidisciplinary Design Optimization: An Emerging New Engineering Discipline," in *Advances in Structural Optimization*, vol. 25, J. Herskovits, Ed., in Solid Mechanics and Its Applications, vol. 25. , Dordrecht: Springer Netherlands, 1995, pp. 483–496. doi: 10.1007/978-94-011-0453-1_14.

[19] C.-T. Su and L.-I. Tong, "Multi-response robust design by principal component analysis," *Total Qual. Manag.*, vol. 8, no. 6, pp. 409–416, Dec. 1997, doi: 10.1080/0954412979415.

[20] L.-I. Tong, C.-H. Wang, and H.-C. Chen, "Optimization of multiple responses using principal component analysis and technique for order preference by similarity to ideal solution," *Int. J. Adv. Manuf. Technol.*, vol. 27, no. 3–4, pp. 407–414, Jul. 2004, doi: 10.1007/s00170-004-2157-9.

[21] N. C. Brown, J. I. F. de Oliveira, J. Ochsendorf, and C. Mueller, "Early-stage integration of architectural and structural performance in a parametric multi-objective design tool," Jul. 2016, doi: 10.1201/b20891.

[22] N. C. Brown and C. T. Mueller, "Design variable analysis and generation for performance-based parametric modeling in architecture," *Int. J. Archit. Comput.*, vol. 17, no. 1, pp. 36–52, Mar. 2019, doi: 10.1177/1478077118799491.

[23] P. Tanskanen, "The evolutionary structural optimization method: theoretical aspects," *Comput. Methods Appl. Mech. Eng.*, vol. 191, no. 47–48, pp. 5485–5498, Nov. 2002, doi: 10.1016/S0045-7825(02)00464-4.

[24] K. Yonekura and O. Watanabe, "A Shape Parameterization Method Using Principal Component Analysis in Applications to Parametric Shape Optimization," *J. Mech. Des.*, vol. 136, no. 12, p. 121401, Dec. 2014, doi: 10.1115/1.4028273.

[25] American National Standards Institute, "Standard for Performance-Rated Cross-Laminated Timber." 2019.

[26] "Minimum Design Loads and Associated Criteria for Buildings and Other Structures ASCE/SEI 7-22." doi: https://doi.org/10.1061/9780784415788.